# MODELING OF OVERFLOW CURVE IN URBAN MANAUS RIVERS

**Andréia Rodrigues Gomes1**
Paulista University (UNIP) - Manaus-AM, Brazil.
arodriguesm.eng@gmail.com

**Alexandra Amaro de Lima2**
Research department, Galileo Institute of Technology and Education of the Amazon – ITEGAM.
Manaus-AM, Brazil.
Paulista University (UNIP) - Manaus-AM, Brazil.
xanduca@gmail.com

**Raylla Carvalho3**
Paulista University (UNIP) - Manaus-AM, Brazil.
reylla.carvalho@gmail.com

**Igor Felipe Oliveira Bezerra4**
Research department, Galileo Institute of Technology and Education of the Amazon – ITEGAM.
Manaus-AM, Brazil.
igor.oliveira@itegam.org.br

**Jorge de Almeida Brito Júnior5**
Research department, Galileo Institute of Technology and Education of the Amazon – ITEGAM.
Manaus-AM, Brazil.
Paulista University (UNIP) - Manaus-AM, Brazil.
jorge.brito@itegam.org.br

## ABSTRACT

*The monitoring of water bodies is of great importance in urban areas, and also in the economic and social context of the large Brazilian metropolises. Urbanization alters the flow of rivers and streams that cut through large urban areas. At the same time, river monitoring can be performed using the mathematical methods present in the literature. This work will show the overflow curve of streams that cross the central areas of the city of Manaus, being possible to visualize through satellite images. For the characterization of the basins, besides satellite images, precipitation time series are used around the studied areas. With the data obtained from the study, it is expected to generate a program that warns the riverine population, for possible floods before they occur. It is also possible to develop a program that calculates a new gutter profile, which includes the design flow, for the studied streams.*

**Keysword:** Overflow curve, urban floods, monitoring risk areas.

## 1. INTRODUCTION

Population increase in large Brazilian cities has been significantly over the last decades. In Brazil, according to data from the Brazilian Institute of Geography and Statistics (IBGE), in the 1940s, the population living in urban areas was smaller. The urbanization process became notorious since the 1960s, especially in the northern states, Acre, Amapá, Amazonas, Pará, Rondônia and Roraima as (BROWDER and GODFREY, 1990, 1997; BROWN et. Al., 1994). In the state of Amazonas, the implementation of the Manaus Free Zone was fundamental for the exponential increase of urbanization (OLIVEIRA and SCHOR, 2009).

The growth of cities causes a serious of environmental impacts such as deforestation, landslides and extreme weather events (OJIMA, 2011; OWEN, 2009; TUCCI, 2007). One of the main problems affecting urban areas is the large volumes of water generated by rainfall and the effect of soil sealing. Urban spaces that do not have adequate rainwater disposal components suffer from frequent flooding, causing environmental, social and economic problems.

According to PHILIPPI (2005), urban floods are caused mainly by the excess runoff, caused by the high impermeability factor that prevents the infiltration of these waters in the soil, thus, when the runoff volume exceeds the design runoff competence, the floods occur. (JONOV et. Al., 2013).

According to the Manaus City PDUA, uncovered and permeable areas are defined so that these same areas do not present any constructive alteration. Population expansion has spread horizontally in the peripheral regions, more precisely to the North and East Zones of the city of Manaus.

The monitoring of water bodies is of paramount importance in urban areas, this applies in the economic and social context of the city, as urbanization in a way alters the flow of rivers and streams that cut through the large metropolises. In addition, urban areas are susceptible to extreme precipitation events, which associated with soil sealing in these areas can lead to increased level of streams causing damage to surrounding areas (BARROS and CONDE, 2017; SILVA et al., 2018). The stream 40, Bindá, and Mindu, are located in the urban area and most susceptible to flooding in the city of Manaus, and for this reason, monitoring these can help the population and public agencies of the city.

One way to monitor urban rivers and streams is through hydrological models. The more robust the model is, the more viable its implementation can become (ZHANG & PAN, 2014; MONTE et al., 2016). Hydrological models can estimate impermeable areas and, at the same time, relate to urban areas (TUCCI, 2000). In addition, it is possible to simulate the effects of precipitation on river flow, infiltration and surplus through runoff (TUCCI, 2000; 2007). Thus, this article will try to obtain an overflow curve through precipitation information for three urban streams in Manaus / AM.

## 2. METHODOLOGY

To obtain the flooding area in the Manaus Igarapés Urban basins, it will be necessary to obtain the total area of the basins. This area will be measured by drawing contour lines (water dividers) using the ArcGIs MAps program, student version, as a tool. On-site visits will be made to the selected igarapés basins, with collections of the physical characteristics of the watercourses in 20m by 20m stakes, where the images describing the region were cataloged, as well as information obtained from the residents, location geographic and satellite quotas. To obtain the flow calculation of the Basin, the mapping data from the Manaus City Hall database, available on a digital platform, will be used. The data of dimension, extension, tributaries and area will be obtained using the software ArcGIs Maps, student version. Once the in situ information is collected, it will be tabulated for applying the basin calculation methodology.

For the characterization of the rainfall regime will be made annual precipitation averages, from information will be taken from the database of the National Institute of Meteorology - INMET, the stations closest to the areas of the basins under study, formulating the rain equation (IDF curve). In the study region.

From the rainfall data will be constructed the series of probable annual maximum heights and respective Recurrence Time (Tr) and associated probability, which will result in the probable maximum heights for return periods of 10 to 100 years.

Also, it will be possible to obtain the maximum probable heights (h) for durations (t), which can also be obtained the maximum probable intensities (i) for periods (t) of 5, 10, 15, 20, 25. and 30 minutes and 1, 6, 8, 10, 12 and 24 hours. Finally, with the obtained results, it will be possible to find the IDF curve for the study region, given by Equation 1.0:

$$i = \frac{18{,}12691 \, . Tr^{0{,}105789}}{(t + 9{,}788612)^{0{,}724313}} \quad (1.0)$$

Drainage structures, ie places where flow rates will be determined by the rational method, rainfall duration is also the concentration time, valid for basins with drainage areas up to 100 hectares, with tc in minutes (equation 2.0). Subsequently, it will be possible to obtain flow calculations, where for a drainage basin in the less than 50 ha (0.5 km2), with a short concentration time, the Rational Method (equation 3.0) will be used directly.

$$tc = 57\left(\frac{L^3}{H}\right)^{0{,}385} \quad (2.0)$$

$$Q = \frac{\text{C.i.A}}{6} \quad (3.0)$$

Where: "C" is the surface runoff coefficient obtained from field information (NETTO and FERNÁNDEZ, 2018). Also, the surface runoff values in areas with surface coverage and divergent characteristics, as shown by NETTO and FERNÁNDEZ (2018). Also, for the project flow rates, and for verifying the existing talveg crossings, a value of 0.70 was initially found for the surface runoff coefficient, which was corrected for Macrodrainage through Equation 4.0.:

$$C_{Tr} = 0{,}8 \, . \, T_r^{0{,}1} . \, C_{10} \quad (4.0)$$

Where: C10, the value of 0.70 is used, which was determined from the average between the coefficients "C10" and "C50". To determine the degree of soil impermeability, it is necessary to know its use, where it can be classified as low, medium and high. This knowledge of land use is obtained through the degree of urbanization, vegetation cover and soil type, which are the same used in NETTO and FERNÁNDEZ (2018). In this study, the value of n = 0 was used. Finally, the flood flow is determined and added to the value obtained from the base flow. The latter was admitted to be in the order of 10%, from which the maximum project flow rate is obtained.

Thus, the flood curves were drawn, and the cross-sections of the studied water bodies were chosen and for the on-site collection points every 20m. To draw the flood curves, a maximum rainfall intensity is chosen for the region, so it will be possible to simulate an atypical rainfall and predict the area of flooding. Once the maximum flow rate of the basin is available, and knowing from the field data collected on site, the cross section of the existing watercourses, it will be possible to obtain the maximum water level quota for the cross section (equation 5.0).

$$A.R^{\frac{2}{3}} = \frac{Q}{K.J^{1/2}} \qquad (5.0)$$

Finally, it was possible to predict the maximum water depth, so that it was possible to integrate all the 20m points into 20m and to draw the flooding (possibly) overflow in the basins. With this curve is possível visualizar, através satellite images, the locations that will be affected by the intensity of the rain.

## 3. RESULTS

### 3.1 Basin Characteristics

For the characterization of this study, two large fully urban watersheds of the city of Manaus were chosen for their relevance and easily accessible areas.

- Water Course do Binda - Sub Basin 1;
- Water Course do Mindu - Sub Basin 2;

The Igarapé do Bindá Basin (Figure 1a) is located in the São Raimundo Basin, with an area of 9.26 km² and a perimeter of 23.02 km, where its longest stretch has 8,327.48 m. The source of Bindá is located in the Cidade Nova neighborhood, with the following geographical coordinates 3o 02 '10.25 ”S / 59o 59' 51.83” W, elevation elevation of 83.779 m and its exutory 28.526 m. Flowing down into the French stream, its mouth is located at 3o 02 '10.25 ”S / 59o 59' 51.83” W, having a height of 28.526 m, showing a variation of 2 m to 7.5 m in its cross section.

Also inserted in the São Raimundo Basin, the Igarapé do Mindú Basin (Figure 1b) has an area of 59,212,116.53 m² with a perimeter of 43,856.25 m, where its longest stretch has 18,101.53m. Its source with elevation elevation 64,689m 30 01'07.31 ”S / 590 55'29.84” W is in the Cidade de Deus neighborhood, while its 24,069 m exutory at Igarapé do São Raimundo, which later flows into the Rio Negro (30 07'44.74 ”S / 600 02'05.04” W) (IPAAM, 2008). The Mindú Stream has, to its extent, an average width ranging from 3.0m to 20.0m. It represents just over 53.45% of the drainage area of the São Raimundo basin.

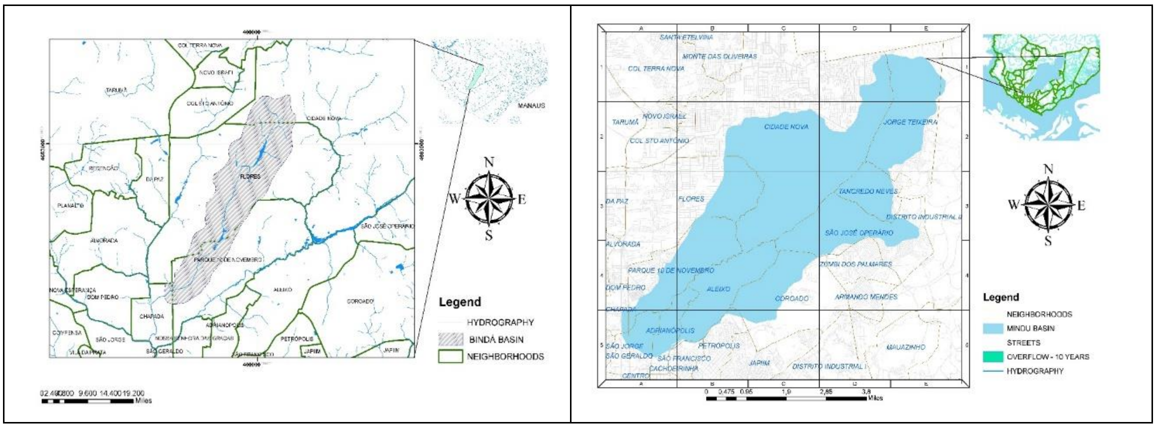


Figura 1: Physical delimitation of the basins: a) Igarapé do Bindá; b) Igarapé do Mindú, in the blue section.

After obtaining the other analysis parameters. With the application of the equations proposed in this study, it was possible to obtain the physical coefficients arranged in Tables 1 and 2, referring to the studied basins.

Table 1 – Study Area Water Course Information of Bindá Water cuorse

| **Physical Characteristics** | **Bindá Water cuorse** |
|---|---|
| **Drainage área** | 9,26Km2 |
| **Perimeter** | 23,02Km |
| **Total Length of Watercourses *** | 17,052Km |
| **Length of Main Watercourse** | 8,33Km |
| **Quota Difference between Headboard and Mouth of the Main Waterway** | 51,68m |
| **Form Factor (Kf)** | 0,13 |
| **Coefficient of Compactness (Kc)** | 2,12 |
| **Drainage Density** | 1,84Km/Km2 |
| **Mean Surface Runoff Length** | 136m |
| **Main Alve declivity** | 0,0062m/m |
| **Concentration Time** | 2,4h |

* Only the perennial water courses

Table 2 – Study Area Water Course Information of Water Course do Mindú

| **Physical characteristics** | **Water Course do Mindú** |
|---|---|
| **Drainage Area** | 59,212Km2 |
| **Perimeter** | 43,86Km |
| **Total Length of Watercourses *** | 103,155Km |
| **Length of Main Watercourse** | 18,51Km |

| | |
|---|---|
| **Quota Difference between Headboard and Mouth of the Main Waterway** | 40,62m |
| **Form Factor (Kf)** | 0,17 |
| **Coefficient of Compactness (Kc)** | 0,41 |
| **Drainage Density** | 1,74Km/Km2 |
| **Mean Surface Runoff Length** | 143,50m |
| **Main Alve declivity** | 2,19m/m |
| **Concentration Time** | 1,77 |

* Only the perennial watercourses

The research will be considered as macrodrainage, so the return period of 10 and 50 years will be adopted.

Applying Equation 4.0, with Tr = 10 and 50 years and C10 = 0.70, the coefficients “C10” and “C50” were determined as an average of 0.77.

For the degree of soil sealing, it is usually adopted n = 0.9. Thus, the maximum design flow is obtained, and with the aid of equation 3.0, of the design flows of the Basins under study. The results obtained are expressed in Tables 3 and 4.

Table 3 – Flow Forecast for the Bindá Basin

| Month | Rain (mm) | m³/s | m³/h |
|---|---|---|---|
| **jan** | 260 | 0,49 | 1772,261111 |
| **feb** | 288 | 0,55 | 1963,12 |
| **mar** | 313 | 0,59 | 2133,529722 |
| **apr** | 300 | 0,57 | 2044,916667 |
| **may** | 256 | 0,48 | 1744,995556 |
| **jun** | 114 | 0,22 | 777,0683333 |
| **jul** | 87 | 0,16 | 593,0258333 |
| **aug** | 58 | 0,11 | 395,3505556 |
| **sep** | 83 | 0,16 | 565,7602778 |
| **oct** | 126 | 0,24 | 858,865 |
| **nov** | 183 | 0,35 | 1247,399167 |
| **dec** | 217 | 0,41 | 1479,156389 |
| **Average Flow (m³/s)** | | **0,36** | **1.297,95** |

Table 4 – Flow Forecast for the Mindú Basin

| Month | Rain (mm) | m³/s | m³/h |
|---|---|---|---|
| **jan** | 260 | 3,150 | 11340,93479 |
| **Feb** | 288 | 3,490 | 12562,26623 |
| **mar** | 313 | 3,792 | 13652,74073 |
| **Apr** | 300 | 3,635 | 13085,69399 |

| | | | |
|---|---|---|---|
| **May** | 256 | 3,102 | 11166,45887 |
| **Jun** | 114 | 1,381 | 4972,563716 |
| **Jul** | 87 | 1,054 | 3794,851257 |
| **Aug** | 58 | 0,703 | 2529,900838 |
| **Sep** | 83 | 1,006 | 3620,375337 |
| **Oct** | 126 | 1,527 | 5495,991475 |
| **Nov** | 183 | 2,217 | 7982,273333 |
| **Dec** | 217 | 2,629 | 9465,318652 |
| **Average Flow (m³/s)** | | **2,31** | **8.305,78** |

For the months of highest rainfall, the Bindá Basin has the average flow rate in its outflow of 0.59 m³ / s and for those with the lowest rainfall 0.11 m³ / s, as shown in Figure 2. The average flow rate of this Water Course is of 0.36 m³ / s. In the Mindú Basin, for the most precipitation months, the average flow in its exsutory is 2.31 m³ / s. As shown in Figure 3.

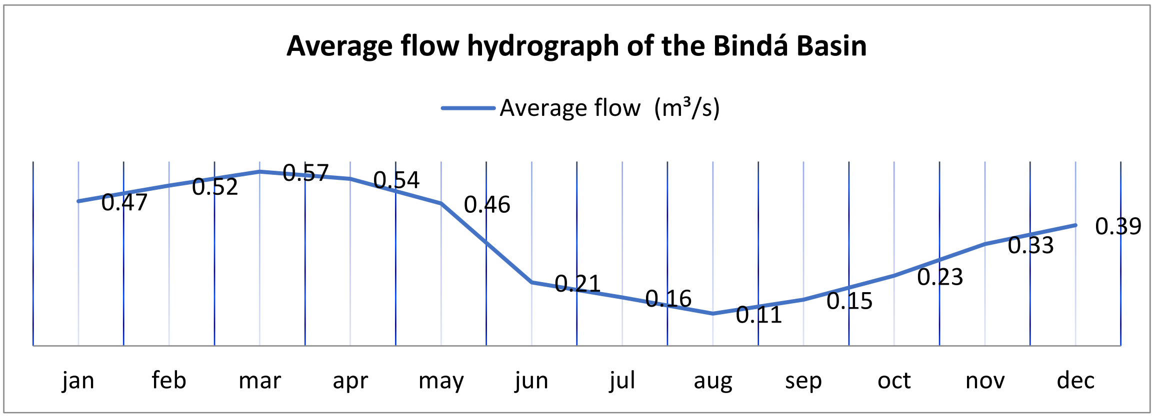


Figure 2 – Average flow hydrograph of the Bindá Basin. Source: own author.

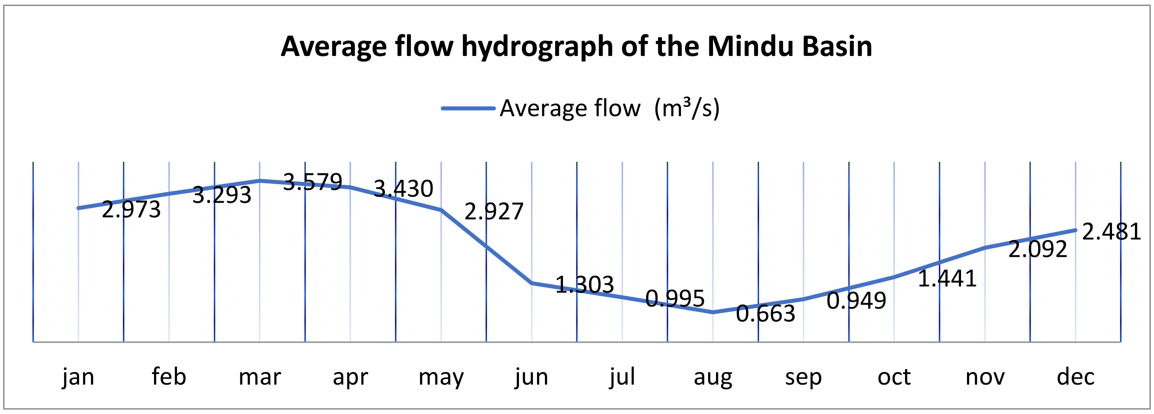


Figure 3 – Mean Flow Hydrograph of the Mindu Basin. Source: own author.

### 3.2 Field survey

Because they are large basins, sections of each densely urbanized Water Course were chosen, inserted in urban areas, for each field survey.

For Igarapé do Bindá, a field visit was made on January 16, 2019 to characterize the body of water in a small stretch of the Water Course, which characterizes a concentration urban area Approximately 1.0 km from the Bindá Water Course, between Rua 13A and near the F, in the November 10th Park neighborhood, as shown in Figure 4a. Information was collected at 10 points downstream of the Water Course at points P-1 through P-10, as shown in Figure 4a.

For the Igarapé do Mindú, a tributary, called São Sebastião Water Course, was chosen in the Parque 10 Neighborhood. Figure 4b illustrates the Water Course sub-basin. On May 15 and 16, a field visit was carried out to characterize the existing body of water in the project area. It was characterized approximately 2.1Km of the São Sebastião Water Course, between the streets Luís Otávio, closest to its source Rua Cel Ferreira de Araújo, called Project, where information was collected in 14 points, upstream of the Water Course, at points P-1 through P-14, as shown in figure 4b.

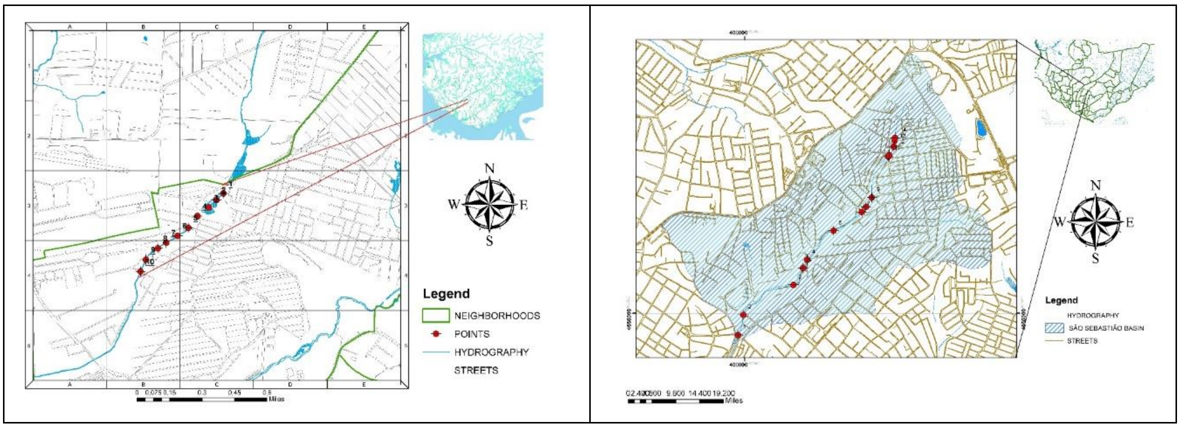


Figure 4: Delimitation of Points: a) Bindá Igarapé Sub Basin; b) Mindú Igarapé Sub Basin.

### 3.3 Flood curves

To generate the rain calculation parameters, the MANAUS rainfall station, which is part of the INMET (National Institute of Meteorology) network, operated since 01/01/1961, was selected. Data were obtained for the period from 1978 to 2018, data used to trace the flood curves of the two basins under study, which are shown in Table 5.

Table 5 – Data of the Maximum Maximum Precipitation Year, in mm, of the Rain Station Manaus, INMET.

| Year | Máximum [mm] | Year | Minimum [mm] |
|---|---|---|---|
| **1978** | 150,0 | 1996 | 155,0 |
| **1979** | 135,2 | 1997 | 105,0 |
| **1980** | 82,7 | 1998 | 69,2 |
| **1981** | 114,0 | 1999 | 133,2 |
| **1982** | 93,0 | 2000 | 154,4 |
| **1983** | 161,8 | 2001 | 96,9 |
| **1984** | 87,4 | 2002 | 90,8 |
| **1985** | 87,2 | 2003 | 138,8 |

| | | | |
|---|---|---|---|
| **1986** | 131,8 | 2004 | 116,5 |
| **1987** | 80,6 | 2005 | 71,2 |
| **1988** | 145,6 | 2006 | 97,4 |
| **1989** | 107,2 | 2007 | 76,1 |
| **1990** | 71,0 | 2008 | 84,2 |
| **1991** | 104,5 | 2009 | 72,0 |
| **1992** | 106,5 | 2010 | 132,5 |
| **1993** | 105,2 | 2011 | 116,2 |
| **1994** | 106,7 | 2012 | 85,2 |
| **1995** | 96,2 | - | - |

Source: HidroWeb, National Water Agency.

Using the data from Table 5, the series of probable annual maximum heights and respective Recurrence Time (Tr) and associated probability was constructed, which is shown in Table 6.

Table 6 – Series of Maximum Annual Heights, Tr and Probability.

| Height [mm] | Tr [yeras] | Probability |
|---|---|---|
| **161,8** | 35,00 | 0,029 |
| **155,0** | 17,50 | 0,057 |
| **154,4** | 11,67 | 0,086 |
| **150,0** | 8,75 | 0,114 |
| **145,6** | 7,00 | 0,143 |
| **138,8** | 5,83 | 0,171 |
| **135,2** | 5,00 | 0,200 |
| **133,2** | 4,38 | 0,229 |
| **132,5** | 3,89 | 0,257 |
| **131,8** | 3,50 | 0,286 |
| **116,5** | 3,18 | 0,314 |
| **116,2** | 2,92 | 0,343 |
| **114,0** | 2,69 | 0,371 |
| **107,2** | 2,50 | 0,400 |
| **106,7** | 2,33 | 0,429 |
| **106,5** | 2,19 | 0,457 |
| **105,2** | 2,06 | 0,486 |
| **105,0** | 1,94 | 0,514 |
| **104,5** | 1,84 | 0,543 |
| **97,4** | 1,75 | 0,571 |

| | | |
|---|---|---|
| **96,9** | 1,67 | 0,600 |
| **96,2** | 1,59 | 0,629 |
| **93,0** | 1,52 | 0,657 |
| **90,8** | 1,46 | 0,686 |
| **87,4** | 1,40 | 0,714 |
| **87,2** | 1,35 | 0,743 |
| **85,2** | 1,30 | 0,771 |
| **84,2** | 1,25 | 0,800 |
| **82,7** | 1,21 | 0,829 |
| **80,6** | 1,17 | 0,857 |
| **76,1** | 1,13 | 0,886 |
| **72,0** | 1,09 | 0,914 |
| **71,2** | 1,06 | 0,943 |
| **71,0** | 1,03 | 0,971 |
| **69,2** | 1,00 | 1,000 |

Applying the Normal distribution, the probable maximum heights of 1 day (h) were obtained for the return periods (Tr) of 2, 5, 10, 20, 50 and 100 years. The probable maximum heights (h) were estimated for the durations (t) of 5, 10, 15, 20, 25 and 30 minutes and for 1, 6, 8, 10, 12 and 24 hours. Table 7 shows the Maximum Probable Heights as a function of Duration and Return Period.

Table 7 - Probable Maximum Height

| **Duration (min)** | **Tr (years)** | | | | | |
|---|---|---|---|---|---|---|
| | 2 | 5 | 10 | 20 | 50 | 100 |
| **5** | 12,946 | 15,689 | 17,123 | 18,307 | 19,640 | 20,529 |
| **10** | 20,561 | 24,918 | 27,196 | 29,077 | 31,194 | 32,605 |
| **15** | 26,653 | 32,301 | 35,254 | 37,692 | 40,436 | 42,266 |
| **20** | 30,841 | 37,377 | 40,793 | 43,615 | 46,790 | 48,907 |
| **25** | 34,649 | 41,991 | 45,830 | 48,999 | 52,567 | 54,945 |
| **30** | 38,075 | 46,144 | 50,362 | 53,845 | 57,766 | 60,379 |
| **60** | 51,453 | 62,357 | 68,057 | 72,764 | 78,062 | 81,594 |
| **360** | 88,206 | 106,898 | 116,669 | 124,739 | 133,820 | 139,875 |
| **480** | 95,556 | 115,807 | 126,392 | 135,133 | 144,972 | 151,531 |
| **600** | 100,456 | 121,745 | 132,873 | 142,063 | 152,406 | 159,302 |
| **720** | 104,132 | 126,199 | 137,735 | 147,261 | 157,982 | 165,130 |
| **1440** | 122,508 | 148,470 | 162,041 | 173,248 | 185,862 | 194,271 |

With the probable maximum heights (h) for durations (t) of 5, 10, 15, 20, 25 and 30 minutes and 1, 6, 8, 10, 12 and 24 hours, the probable maximum intensities (i) were calculated. , for the same durations (t) of 5, 10, 15, 20, 25 and 30 minutes and 1, 6, 8, 10, 12 and 24 hours, shown in Table 8, given by the ratio of heights to duration times.

Tabela 8 - Probable Maximum Intensity

| Duration (min) | Return Period (years) | | | | | |
|---|---|---|---|---|---|---|
| | 2 | 5 | 10 | 20 | 50 | 100 |
| **5** | 2,5891258 | 3,137823 | 3,424636 | 3,661492 | 3,928072 | 4,105793 |
| **10** | 2,0560705 | 2,491800 | 2,719564 | 2,907655 | 3,119351 | 3,260483 |
| **15** | 1,7768511 | 2,153408 | 2,350241 | 2,512788 | 2,695736 | 2,817701 |
| **20** | 1,5420529 | 1,868850 | 2,039673 | 2,180741 | 2,339513 | 2,445362 |
| **25** | 1,3859438 | 1,679658 | 1,833188 | 1,959975 | 2,102674 | 2,197807 |
| **30** | 1,2691793 | 1,538148 | 1,678743 | 1,794849 | 1,925525 | 2,012644 |
| **60** | 0,8575536 | 1,039289 | 1,134286 | 1,212736 | 1,301031 | 1,359894 |
| **360** | 0,2450153 | 0,296940 | 0,324082 | 0,346496 | 0,371723 | 0,388541 |
| **480** | 0,1990749 | 0,241264 | 0,263316 | 0,281528 | 0,302025 | 0,315690 |
| **600** | 0,1674271 | 0,202909 | 0,221456 | 0,236772 | 0,254011 | 0,265503 |
| **720** | 0,1446271 | 0,175277 | 0,191298 | 0,204529 | 0,219420 | 0,229347 |
| **1440** | 0,0850748 | 0,103104 | 0,112528 | 0,120311 | 0,129071 | 0,134910 |

With the obtained results, the IDF curve was formulated for the study regions. For the basins under study, these values are different because they are sub-basins delimited along every 20 m in the study area, where the average tc of 70.04 min is determined for their similar characteristics. The 25-year payback period was adopted because it is macrodrainage. The design precipitation intensity for Tr = 25 is given by Equation 3, where Tr = 10 and 50 and t = tc = 70,04 for both basins.

Table 9 and 10 present the summary of the project flow calculation for the Bindá and Mundú project areas, respectively.

Table 9 – Project Flows (Q) of Bindá Wather Course

| EST | Point | Bi | H | H lâmina (10 year rain) | H lâmina (50 year rain) | Q PROJ (10 year) | Q PROJ (50 yars) |
|---|---|---|---|---|---|---|---|
| **0** | 1,00 | 7,93 | 2,26 | 6,64 | 7,61 | 118,94 | 136,4299 |
| **0+5** | 2,00 | 8,30 | 2,80 | 5,27 | 6,05 | 122,51 | 140,516 |
| **0+10** | 3,00 | 9,20 | 2,73 | 4,95 | 5,68 | 124,29 | 142,5591 |
| **0+15** | 4,00 | 9,00 | 2,73 | 5,13 | 5,89 | 126,07 | 144,6021 |

| | | | | | | | |
|---|---|---|---|---|---|---|---|
| **0+20** | 5,00 | 9,00 | 2,60 | 5,46 | 6,27 | 127,85 | 146,6452 |
| **0+25** | 6,00 | 13,22 | 2,95 | 3,32 | 3,81 | 129,63 | 148,6883 |
| **0+30** | 7,00 | 8,34 | 3,00 | 5,25 | 6,02 | 131,41 | 150,7313 |
| **0+35** | 8,00 | 8,83 | 2,90 | 5,20 | 5,97 | 133,19 | 152,7744 |
| **0+40** | 9,00 | 9,00 | 3,00 | 5,00 | 5,73 | 134,98 | 154,8174 |
| **0+45** | 10,00 | 9,00 | 2,42 | 6,28 | 7,20 | 136,76 | 156,8605 |

Table 10 – Project Flows of the Mindu Basin, Subbasin São Sebastião Water Course.

| **EST** | **Score** | **Bi (m)** | **H (m)** | **H lâmina- (m) - (rain 10 years)** | **H lâmina- (m) - (rain 50 years)** | **Q PROJ- (m³/s) - (10 years)** | **Q PROJ - (m³/s) - (50 years)** |
|---|---|---|---|---|---|---|---|
| **0** | (0-1) | 1,00 | 0,80 | 0,96 | 1,26 | 5,62 | 7,88 |
| **0+100** | (1-2) | 1,00 | 0,80 | 1,31 | 1,76 | 8,26 | 11,58 |
| **0+200** | (2-3) | 1,00 | 0,80 | 1,72 | 2,32 | 11,31 | 15,86 |
| **0+300** | (3-4) | 1,00 | 0,80 | 2,05 | 2,78 | 13,82 | 19,39 |
| **0+400** | (4-5) | 1,00 | 0,80 | 2,50 | 3,41 | 17,26 | 24,21 |
| **0+500** | (5-6) | 1,00 | 0,80 | 3,01 | 4,11 | 21,13 | 29,64 |
| **0+600** | (6-7) | 1,00 | 0,80 | 3,51 | 4,82 | 25,03 | 35,11 |
| **0+700** | (7-8) | 1,00 | 0,80 | 4,25 | 5,85 | 30,73 | 43,10 |
| **0+800** | (8-9) | 1,00 | 0,80 | 4,85 | 6,68 | 35,35 | 49,59 |
| **0+900** | (9-10) | 1,00 | 0,80 | 5,66 | 7,81 | 41,63 | 58,39 |
| **1+00** | (10-11) | 1,35 | 1,50 | 4,04 | 5,52 | 46,81 | 65,66 |
| **1+100** | (11-12) | 1,03 | 1,20 | 6,77 | 9,37 | 52,74 | 73,97 |
| **1+200** | (12-13) | 1,35 | 0,99 | 4,91 | 6,74 | 57,90 | 81,21 |
| **1+300** | (13-14) | 1,40 | 0,85 | 4,86 | 6,66 | 60,61 | 85,01 |
| **1+400** | (14-15) | 1,70 | 0,85 | 3,89 | 5,28 | 64,31 | 90,19 |
| **1+500** | (15-16) | 6,00 | 1,58 | 1,08 | 1,36 | 68,46 | 96,02 |
| **1+600** | (16-17) | 10,00 | 1,78 | 0,76 | 0,95 | 71,58 | 100,40 |
| **1+700** | (17-18) | 8,00 | 2,20 | 0,93 | 1,16 | 76,04 | 106,65 |
| **1+800** | (18-19) | 4,00 | 1,70 | 1,71 | 2,20 | 79,95 | 112,13 |
| **1+900** | (19-20) | 4,00 | 1,50 | 1,75 | 2,26 | 82,70 | 116,00 |
| **2+00** | (20-21) | 2,50 | 1,20 | 3,24 | 4,33 | 93,57 | 131,25 |
| **2+100** | (21-22) | 4,00 | 1,20 | 1,99 | 2,57 | 98,16 | 137,68 |
| **2+200** | (22-23) | 10,00 | 2,21 | 0,93 | 1,21 | 104,86 | 147,08 |
| **2+217** | (23-24) | 10,00 | 2,21 | 2,03 | 2,41 | 96,31 | 135,08 |

Figures 5 and 6 show the overflow of the Bindá and Mindú Water Course gutters, in the sections studied for a 10 and 50 year project rain.

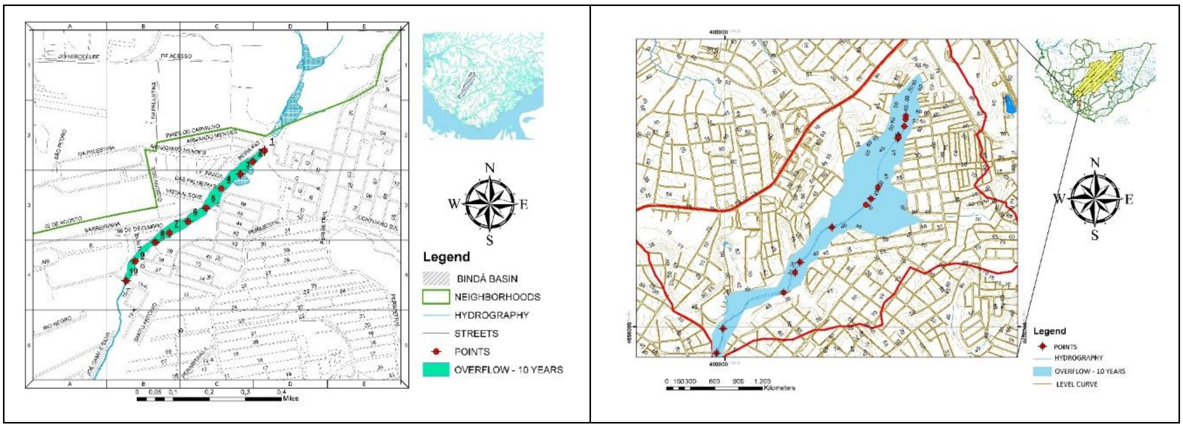


Figure 5: Delimitation of Points: a) Bindá Igarapé Sub Basin for 10-year rain; b) Mindú Igarapé Basin for 10-year rain.

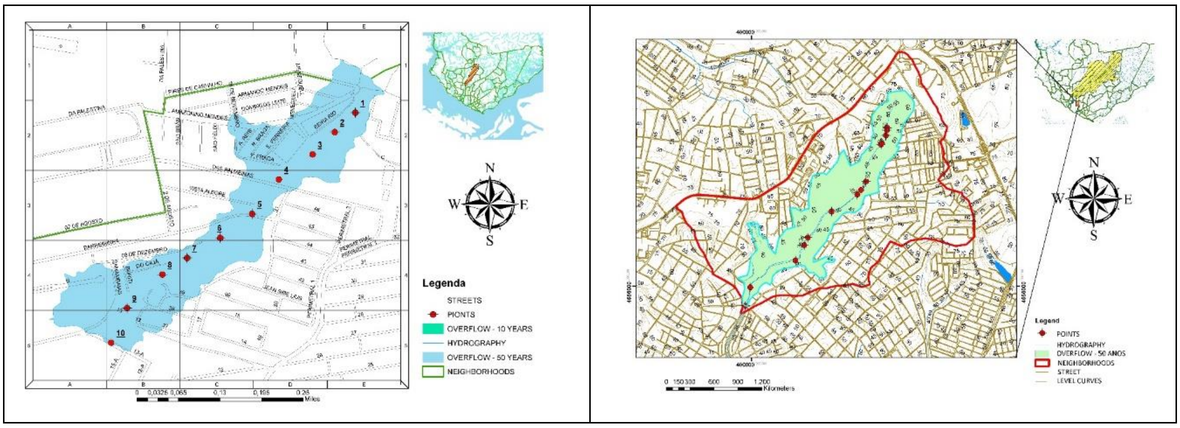


Figure 6: Delimitation of Points: a) 50-year-old Bindá Igarapé Sub-Basin for Rain; b) 50-year-old Rainwater Igarapé Sub Basin.

## 4. DISCUSSION

The physical coefficients of the studied basins indicate a good drainage capacity, but subject to peak flow due to intense precipitation due to its low concentration time.

The regions of the project are inserted in the same urban ecosystem of the city of Manaus has the same climatic characteristics of the rest of the city. However, the flood and ebb regime has no influence on the water levels of the Water Courses under study that are subject to the flow regime due specifically to the rainfall regime, as studied and shown in tables 3 and 4.

Overflowing of the gutters, caused by excessive soil sealing, generate high coefficients of return of water flow to the streams of the streams, which do not support the flow. A possible solution would be the widening and deepening of these channels, generating flow areas for the peak flow.

Figures 5 and 6 show a significant increase in the flooding area only with the change in rainfall recurrence time, also observed in field visits. It is observed that for a normal rainfall, with Tr = 10, the stream does not overflow, as opposed to Tr = 50, impacting a larger number of dwellings.

With the data obtained from the study, it is expected to generate a program that warns the riverine population, for possible floods before they occur. It is also possible to develop a program that calculates a new gutter profile, which includes the design flow, for the studied streams.

## 5. BIBLIOGRAPHIC REFERENCES

Barros, M. T. L. and Conde F. 2017. Urban Flood Warning Systems Social Benefits. World Environmental and Water Resources Congress Sacramento, USA. DOI: 10.1061/9780784480601.054

Brown, L.A., Sierra, R., Digiacinto, S. and Smith, W.R. (1994) Urban-system evolution in frontier settings. *Geographical Review,* 84**(**3)**,** 249–264.

BROWDER, J. O., and GODFREY, B. J. 1990. Frontier urbanization in the Brazilian Amazon: a theoretical framework for urban transition. *Yearbook - Conference of Latin Americanist Geographers*, 16, 56-66.

BROWDER, J. O., and GODFREY, B. J. 1997. *Rainforest cities*. New York: Columbia University Press.

DE INFORMAÇÕES HIDROLÓGICAS–HIDROWEB, ANA Sistemas. Agência Nacional de Águas. 2017. 2017.

GRIBBIN, J. E. 2012. Introdução a hidráulica, hidrologia e gestão de águas pluviais. 4º edição tradução Norte-americana. São Paulo, editora Cengage Learning.

INMET, INDEM. Banco de Dados Meteorológicos para Ensino e Pesquisa. 2012.

JONOV, C. M. P.; NASCIMENTO, N. de O.; PAULA E SILVA, A. de. 2013.Avaliação de danos às edificações causados por inundações e obtenção dos custos de recuperação. Ambiente Construído, Porto Alegre, v.13, n.3, p.75-94, jan./mar.

Município de Manaus. 2011. Secretaria Municipal de Infraestrutura, Plano Diretor de Drenagem Urbana de Manaus. Manaus, CONCREMAT Engenharia.

NETTO, Azevedo; Y FERNÁNDEZ, Miguel Fernández. Manual de hidráulica. Editora Blucher, 2018.

OJIMA, R. 2011. As dimensões demográficas das mudanças climáticas: cenários de mudança do clima e as tendências do crescimento populacional. Revista Brasileira de Estudos de População, v. 28, n. 2, p. 389-403.

OLIVEIRA, J. A. e SCHOR, T. 2009. "Manaus: transformações e permanências, do forte à metrópole regional". In: CASTRO, E. (org.). *Cidades na floresta*. São Paulo, Annablume.

MONTE, B.E.O.; COSTA, D.D.; CHAVES, M.B.; MAGALHÃES, L.O.; UVO, C.B. 2016. Hydrological and hydraulic modelling applied to the mapping of flood-prone áreas. *Revista Brasileira de Recursos Hídricos*, 21: 152-167.

PHILIPPI, A. J. R. 2005. Saneamento, saúde e ambiente: fundamentos para um desenvolvimento sustentável. 2º Coleção. Barueri, São Paulo, editora Manole.

SILVA, C.V.F.; SCHARDONG, A.; GARCIA, J.I.B. and OLIVEIRA, C. de P.M. 2018. Climate change impacts and flood control measures for highly developed urban watersheds. Water (Switzerland), 10 (7):1–18.

TUCCI, C. E. M. and PORTO, R. L. (2000). Storm hydrology and urban drainage. In: Tucci, C. Humid Tropics Urban Drainage, cap. 4. UNESCO.

TUCCI, C. E. M. 2007. Inundações urbanas. Porto Alegre: ABRH/RHAMA.

ZHANG, S. PAN, B. 2014. An urban storm-inundation simulation method based on GIS. Journal of Hydrology, 517:260–268.